# Titania−Hydroxypropyl Cellulose Thin Films for the Detection of Peroxide Vapors

Travis H. James,[†] Cody Cannon,[†] Dane Scott,[†] Zeid AlOthman,[‡] Allen Apblett,[†] and Nicholas F. Materer*,[†]

[†]Department of Chemistry, Oklahoma State University, Stillwater, Oklahoma 74078-3071, United States
[‡]Chemistry Department, College of Science, King Saud University, Riyadh 11451, Kingdom of Saudi Arabia

Ⓢ *Supporting Information*

**ABSTRACT:** Titania nanoparticles in a hydroxypropyl cellulose matrix produced using a sol−gel method were utilized to prepare films on polycarbonate slides and coatings on cellulose papers. The exposure of these materials to hydrogen peroxide gas leads to the development of an intense yellow color. By using an inexpensive web camera and a tungsten lamp to measure the reflected light, first-order behavior in the color change was observed when exposed to peroxide vapor of less than 50 ppm. For 50 mass percent titania nanoparticles in hydroxypropyl cellulose films on polycarbonate, the detection limit was estimated to be 90 ppm after a 1 min measurement and 1.5 ppm after a 1 h integration. The coatings on the filter paper had a 3-fold higher sensitivity compared to the films, with a detection limit of 5.4 ppm peroxide for a 1 min measurement and 0.09 ppm peroxide for a 1 h integration. The high sensitivity and rapid response of these films make them a promising material for use as a sensitive peroxide detector.

**KEYWORDS:** *titania, sol−gel, peroxide vapor, thin film sensor, hydroxypropyl cellulose*
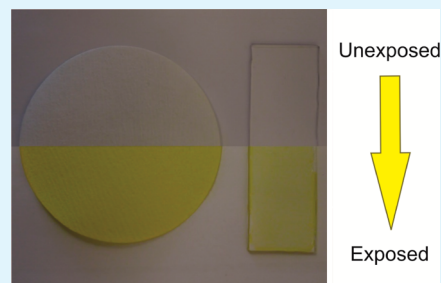
## INTRODUCTION

Peroxides ($O_2^{2-}$) are extremely strong oxidizing agents of great importance in many industrial and biological fields. The most prominent of these oxidants, hydrogen peroxide ($H_2O_2$), is useful as a bleaching agent in the paper and textile industries, which together consume over half of the annually produced supply,[1,2] and as a reagent for the treatment of organic and other pollutants in water supplies.[3,4] Gaseous hydrogen peroxide is often used in the food and medicinal fields as a cleaning reagent in situations where a sterile environment with no bacterial or microbial growth is essential.[5−11] Due to its strong oxidizing potential, the Occupational Safety and Health Administration (OSHA) has set a permissible average exposure limit of 1 ppm over an 8 h day,[12] which leads to the requirement that users must be able to constantly monitor levels of hydrogen peroxide down to 1 ppm. OSHA-approved methods for quantification of gaseous peroxide include drawing the atmosphere in question through an acidified solution of titanium oxide sulfate[13] and the use of Dräger or similar tubes specific for hydrogen peroxide.[14] In the first case, an optical measurement of the solution is used to determine the peroxide concentration; in the latter case, colored bands form, and the length of these bands correlates with the concentration. Additional methods for peroxide detection and quantification include fluorometry,[15−18] amperometry,[19−22] spectroscopy,[23−26] and electrochemical sensing.[27] Many of these methods cannot be easily automated because they require preconcentra-tion of the atmosphere in solution and some amount of wet chemistry or require constant attention by a technician.

Nanoparticle titanium dioxide (i.e., titania nanoparticles) has gained interest as a catalyst and gas sensor. Beginning with its use by Fujishima and Honda as a catalyst for the photolysis of water,[28] titania nanoparticles have been used in solar cells,[29−31] UV filters,[32,33] and water purification technology.[34] As sensors, they have application for the detection of hydrogen sulfide,[35] ethanol,[36] and carbon monoxide among many other gases.[37−39] One notable paper used $Ti^{3+}$-doped $TiO_2$ spherelike nano-particles for solution-based hydrogen peroxide detection.[40] As solid sensors, titania films can be produced by many methods including physical and chemical vapor depositions,[41−48] pyrolysis,[49−51] RF sputtering,[52−54] coprecipitation,[55−57] and sol−gel methods.[58−61] Of these, the sol−gel approach is attractive due to the low temperatures, low cost, and particle size control.

Xu and co-workers have recently presented a cellulose paper method based on aqueous absorption of titanium(IV)-oxo complexes that bind with hydrogen peroxide vapor, causing a color change.[62] Our work complements this study by investigating the use of nanostructured titanium dioxide encapsulated within hydroxypropyl cellulose films supported by polycarbonate slides or cellulose filter papers. The films and

coatings were prepared according to a method previously described by Kusabe and co-workers[63] with the elimination of the final calcination step used to produce pure titania thin films. In terms of detection, this work builds on the OSHA VI-6 method for hydrogen peroxide detection utilizing the complex-ion between $Ti^{4+}$ ions (in this case titanium(IV) oxysulfate) and hydrogen peroxide.[13] Titanium(IV) oxysulfate is believed to be composed of Ti−O−Ti−O− zigzag chains coordinated with water and hydrogen sulfate ions.[64] When reacted with hydrogen peroxide in an acidic media, the complex that is formed can be either mononuclear with one peroxide per titanium ion or dinuclear with peroxides bridging between titanium ions.[65] The selectivity, stability, and final intense color of the resulting titanium(IV)-oxy complexes are the reason these materials are used for colorimetric detection. Vogel's Textbook of Quantitative Chemical Analysis references the use of acidic hydrogen peroxide solution to quantify titanium in solutions.[66] Our sol−gel films and coatings have a similar color change when exposed to peroxide vapors, changing from colorless to yellow, motivating this study. It is anticipated that these films can be integrated into a low-cost sensor to monitor peroxide concentrations in industrial workplaces.

## ■ EXPERIMENTAL DETAILS

**Titanium(IV) Isopropoxide−Cellulose Solution.** A solution of titanium(IV) isopropoxide with hydroxypropyl cellulose in 2-propanol was produced following the procedure outlined by Kusabe and co-workers.[63] Briefly, 1 g of hydroxypropyl cellulose (Alfa Aesar, $M_r$ = 100 000) was dissolved in 70 mL of 2-propanol (Pharmco-Aaper, ACS reagent). A measured amount of titanium(IV) isopropoxide (Alfa Aesar, 97%) was then added dropwise while stirring. After stirring for 1 h under nitrogen, 1.5 g of concentrated hydrochloric acid (Pharmco-Aaper, ACS reagent) diluted with 20 mL of 2-propanol was added to the titanium−cellulose solution. The final solution was stirred under nitrogen for 24 h before use. Solutions with varying quantities of titania were prepared up to the point where sufficient titania was present to yield a 60 mass percent titania/(titania + hydroxypropyl cellulose) film, assuming that the titanium(IV) isopropoxide was completely converted to titania. After production, the solutions were pale yellow and stored under nitrogen. Film preparation was typically performed within 12 h after the initial 24 h mixing period.

**Preparation of the Films and Coatings.** Polycarbonate slides (1 in. × 3 in. × 0.060 in.) were sonicated in ethanol for 30 min and dried in air. Once dried, an excess volume of the titanium(IV) isopropoxide−cellulose solution was applied to a slide held in an aluminum slide holder (0.040 in. deep). A Gardco 8-path wet film applicator was used to remove the excess solution and produce films of the precursor solutions with a homogeneous thickness of 0.020 in. The slides were then placed under a watch glass to air-dry for 1 h. The resulting films were then used as prepared without the implementation of the calcination stage.

Similar coatings were produced on cellulose filter paper (VWR 415) by coating one side of the paper with an equal volume-per-area amount of the titanium isopropoxide−cellulose solution, as was used for the polycarbonate slides. The papers were hung vertically to air-dry for 1 h. In the first 5 min of drying, the filter papers were constantly rotated to ensure a uniform thickness.

**Titanium(IV) Oxysulfate Solution.** The colorimetric procedure developed by OSHA was utilized to measure the peroxide vapor concentration.[13] This method requires a solution of titanium(IV) oxysulfate in sulfuric acid. This was produced by dissolving a mixture of 5.5 g of dehydrated $TiOSO_4 \cdot xH_2O$ (Strem Chemicals) and 20 g of ammonium sulfate (Spectrum, ACS reagent) in a heated solution of 100 mL of sulfuric acid (Pharmco-Aaper, ACS reagent). After cooling, the resulting solution was added to 350 mL of ultrapure water, filtered through a 0.40 $\mu$m filter to remove any suspended materials, and diluted to 500 mL.

**Film Testing Apparatus.** Figure 1 shows a schematic diagram of the apparatus that was used to expose and monitor the films. A
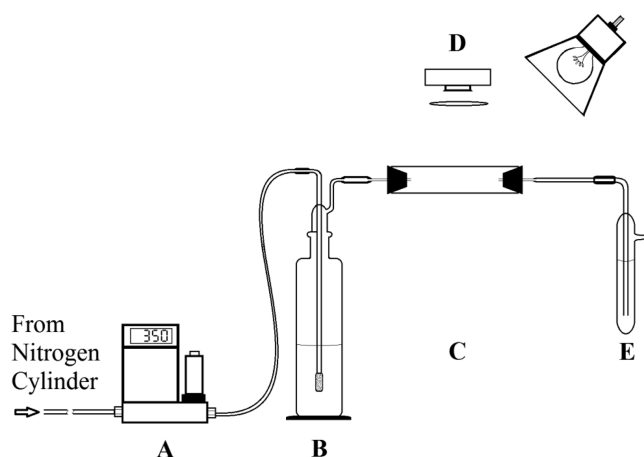


**Figure 1.** Schematic diagram of the apparatus that depicts (A) the flow controller, (B) the bubbler to entrain peroxide vapor, (C) the exposure chamber, (D) the detection system, and (E) a bubbler used to determine the total concentration of peroxide in the flow.

nitrogen cylinder (Airgas, ultrahigh purity) was used to supply nitrogen as the carrier gas. The regulator backing pressure was set to 20 psi, and the flow was fixed at 350 standard cubic centimeters per minute (sccm) for all experiments using an Omega FMA 5500 mass flow controller (A). The nitrogen flow was then directed through a 250 mL bubbler containing peroxide solution (B). The gas was dispersed into the solution using a sintered glass head, which distributed the gas through the solution to ensure a steady uptake of the peroxide vapor. The solution concentration of hydrogen peroxide in the bubbler determines the gas-phase concentration, which is directly measured as described below. Next, the peroxide-enriched gas was directed into a glass cell containing the sample, either a film on a polycarbonate slide or a coating on cellulose filter paper (C). The glass cell had a piece of white paper attached on its outside bottom to create a white background. A 20 W incandescent light was positioned above the cell to provide homogeneous lighting for the slide, and a Logitech Pro 9000 USB camera recorded images of the sample during exposure to peroxide vapor (D). Between the camera and the cell was a Leiz Wetzlar BG 12 blue bandpass filter, which isolated the wavelengths between 300 and 500 nm. After leaving the cell, the gas progressed through a bubbler containing 25 mL of the titanium(IV) oxysulfate solution (E), which reacts with the peroxide in the gas and produces a color change that is proportional to the total quantity of peroxide in the gas. A second bubbler was attached following the first one to confirm complete reaction of entrained peroxide vapor with the titanium(IV) oxysulfate solution. There was no measured absorbance change in the solution of the second bubbler when run with 30% peroxide solution, the highest solution-phase concentration used in these experiments, for 30 min, indicating that the peroxide vapor was completely reacted in the first bubbler. The total peroxide concentration was determined using the OSHA colorimetric method that utilizes the absorption of the titanium(IV) oxysulfate solution at 410 nm.[13] A Cary 50 Bio UV−vis spectrometer was used for the absorption measurement and was calibrated as per this colorimetric method. The peroxide concentration in the gas was computed using the total concentration in titanium(IV) oxysulfate solution, the flow rate which was fixed at 350 sccm for all experiments, and the exposure time of the films to the flowing gas. This process was performed for every exposure to determine the vapor concentration. The referenced OSHA VI-6 method describes the hydrogen peroxide quantification procedure for gas-phase sampling.[13]

The total volume of $N_2$ gas passed through the apparatus is 21 L for an hour long exposure. Since $N_2$ gas bubbles through an aqueous solution of hydrogen peroxide, the addition of water vapor could
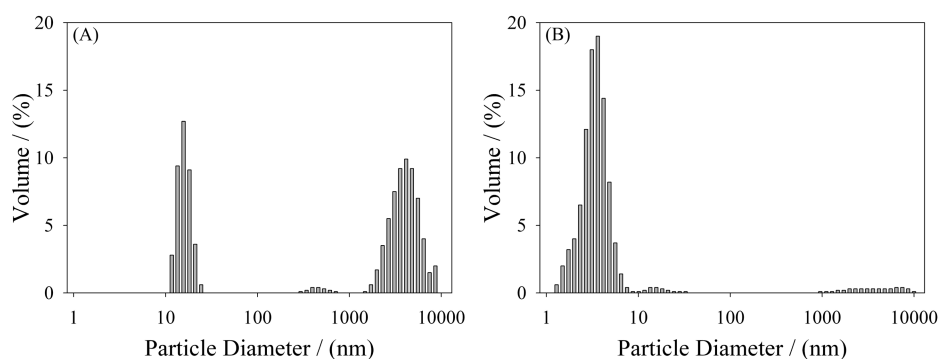
**Figure 2.** DLS analyses of cellulose solution (A) before addition of titanium isoproproxide and (B) immediately after addition of titanium isoproproxide.
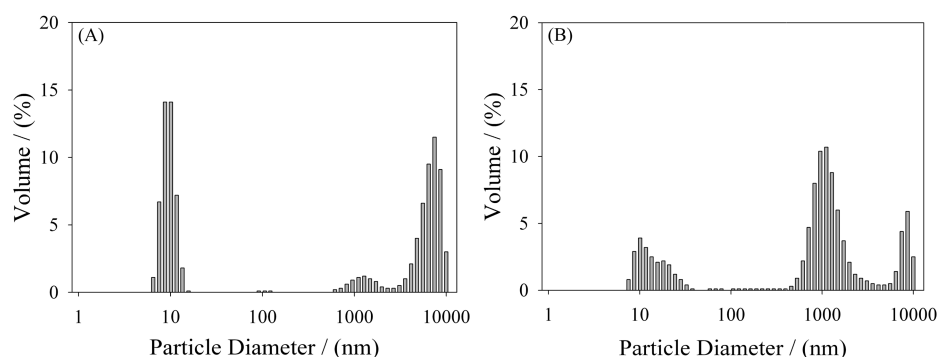


**Figure 3.** DLS analyses of titania−cellulose solution after stirring (A) for 1 day and (B) for 1 week.

slightly increase the total volume of gas volume passed. Since this was not corrected for in the computation of the gas-phase concentration of hydrogen peroxide, a slight underestimation could possibly occur. Running the bubbler for an extended time (18 h) resulted in a water mass loss of 0.5 g/h. This mass of water corresponds to approximately 0.6 L of water vapor in 21 L of $N_2$ gas, given a maximum 3% error toward lower parts per million.

Before each experimental run, the targeted gas-phase concentration was obtained by varying the concentration of hydrogen peroxide in the bubbler solution. For precise values, some iteration is required due to variability in the stock hydrogen peroxide concentration with time. Once started, each exposure was recorded as an MJPG video and saved to a disk. The video was shortened using the open-source program MEncoder by extracting one frame every 10 s for the duration of the exposure, typically 0.5−1 h. Data reduction was performed using ImageJ, an open-source analysis software package developed by the National Institutes of Health.[67] The imported video was split into red, blue, and green channels. As discussed above, the BG 12 blue bandpass filter limited the range of recorded wavelengths from 300 to 500 nm. In these experiments, the reflected light saturated the blue channel; therefore, the red channel, which has much lower sensitivity in the blue region, was used to quantify the reflected light. The response of the red channel to the desired analytical wavelengths was confirmed using a broadband light source and a monochromator. Intensities were extracted from the video using ImageJ. Except when noted, the intensity was determined by an average center section area of the samples, and the results were used to generate all plots.

**Particle Size Measurements.** A Malvern HPP5001 particle size analyzer was used for size characterization of particulates in solution. A total of 25 measurements were performed for each sample, which were undiluted and measured at 25 °C.

## ■ RESULTS AND DISCUSSION

**Characterization of the Films and Coatings.** Films and coatings were prepared as described in the Experimental Details section. As the films air-dried, there was a tendency for the films, produced from the titanium(IV) isopropoxide−cellulose solutions with high titania mass loading, to crack or peel away from the slide. This cracking was especially prevalent for films deposited on glass slides, which led to the use of polycarbonate slides in this investigation. On the polycarbonate substrates, virtually all of the 40 and 50 mass percent titania coatings produced high quality films upon drying. However, films with 60 mass percent titania could not be produced without cracking. The decrease in adherence of the films to the slide with high titania content may be due to the lower hydroxypropyl cellulose content and increased stress within the film, which results in a greater propensity for cracking. These findings are in agreement with the previous description of film cracking at higher titania loadings by Kusabe and co-workers.[63]

Therefore, the majority of the work described herein was performed with films with a 50 mass percent titania loading or lower. The greatest color change was obtained for films and coatings with 50 mass percent titania content. These films also displayed excellent overall stability on the polycarbonate slides before peroxide exposure. Although films with 40 and 50 mass percent titania loading developed stress cracks after reacting with the peroxide vapor, the degree of cracking had little influence on the observed color evolution upon exposure to hydrogen peroxide. There was no observable cracking or peeling of coatings applied on the filter paper.

As the titania−cellulose solutions aged, there was an observable increase in the turbidity of the solution. This increase was attributed to continual particle growth and aggregation with time. Dynamic light scattering (DLS) analysis was used to measure the growth of the titania nanoparticles in freshly prepared solutions as they aged for up to 1 week (see Figures 2 and 3). DLS measurements of the precursor solution

for 50 mass percent titania films were performed immediately (i.e., within 5 min) after preparation and 1 day of mixing.

The hydroxypropylcellulose solution lacking titanium isopropoxide (Figure 2A) showed distributions centered around 12 and 4000 nm, with the larger diameter distribution containing over 60% of the total particle volume. This larger distribution was attributed to the agglomeration of the hydroxypropyl cellulose without a well-defined mean particle size. Upon the addition of titanium isoproproxide, a large distribution centered between 3 and 4 nm appeared, comprising nearly 94% of the measured particle volume (Figure 2B). This distribution was assigned to nanoparticulate titania forming in the solution. The remaining volume was as seen before in the hydroxypropylcellulose control. The population of the nanoparticles in this size range decreased over a 24 h mixing period, by the end of which the mean particle size had increased to approximately 10 nm (Figure 3A). This distribution is noticeably shifted to lower particle sizes, with respect to the hydroxypropylcellulose control. There is also a new, much smaller distribution around 1000 nm or 1 $\mu$m. After 1 week, the titania particles reached a mean size distribution around 1 $\mu$m (Figure 3B). Experimentally, the films made within 24 h of the solution preparation had slightly higher sensitively, or a more rapid color change, to hydrogen peroxide vapor. To maintain consistency, all films and coatings were prepared within 24 h of preparation of the precursor solution.

The films and coatings were also used shortly after preparation to ensure consistency. Over a week, both the films and coatings remain stable. For the films, there is very little difference in the sensitivity between a fresh film and one stored in a covered Petri dish and exposed to light for six months. The dense sol−gel film combined with the lack of water that can produce radicals via photochemistry is believed to contribute to the observed stability. However, the coatings on filter paper are less stable and become brittle with time. Over a six months period in a covered Petri dish, the coatings lose approximately 50% of their initial sensitivity. However, they are still more sensitive than the films even after six months of storage. Although not a focus of this study, it is thought that better storage conditions could extend the lifetime of the coatings.

**Reaction Kinetics.** Upon exposure to gaseous hydrogen peroxide, the films and coatings changed from colorless to yellow wherein the intensities are dependent on the peroxide concentration and the exposure time. When the intensities were examined in detail, it was found that the images initially saturated the blue channel. As the coatings and films react with hydrogen peroxide, the absorption of light between 300 and 500 nm begins to occur (as demonstrated by the UV spectra of exposed films), which causes less light to be reflected and results in a darker image of the film or coating. A control film and coating created without the addition of titanium isopropoxide did not have an observed color change during exposure to peroxide vapors.

The particular red dye used in the web camera has reasonable absorbance in the blue region of the spectra, as confirmed using a broadband light source combined with a $^1/_8$ m monochromator. Therefore, the red channel has an increased dynamic range but lower sensitivity. The resulting image after splitting the color channels using ImageJ and focusing only on the red channel is shown in Figure 4A, B. As can be seen, a dramatic decrease in the intensity was readily observed.
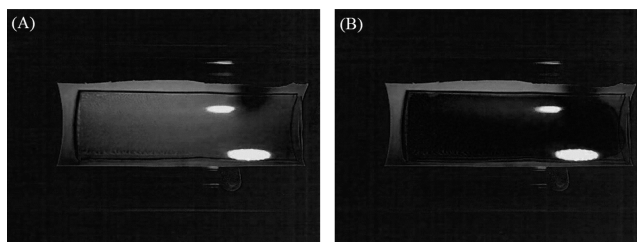


**Figure 4.** Reflected image of a titania−cellulose film on polycarbonate (A) before and (B) after peroxide exposure. The film was exposed to a hydrogen peroxide concentration of 42.1 ppm for 1 h.

As discussed in the Experimental Details section, ImageJ was used to extract the intensity as a function of time from the video. A typical decrease in reflected intensity with time is shown in Figure 5A. The intensity appears to exponentially decline with time or peroxide exposure. This observation was confirmed by plotting the natural logarithm of the intensity versus exposure time (Figure 5B), yielding a linear plot that is characteristic of an exponential time dependence. Additional experimental data can be found in the Supporting Information. Included are an experimental run with 0 ppm hydrogen peroxide, and several different runs with 50 mass percent titania films and coatings at different hydrogen peroxide concentrations.

The negative slope of this plot (Figure 5B), determined by linear regression, is the phenomenological first-order rate constant. At later time points, the decrease in reflected intensity slows and then stops as the active titania particles in the film and coating are consumed. The saturation intensities for 25 and 50 mass percent titania coatings on filter paper were $44.7 \pm 5.5$ and $16.2 \pm 0.3$, respectively. These intensities were determined by the averaging of three experiments, two 60 min exposures to hydrogen peroxide gas with concentrations of 37.3 and 38.5 ppm and one 80 min exposure of 10.7 ppm. The raw saturation intensities for each experiment was performed by averaging of the last 5 min of each exposure and differed by less than 2% from that computed from the previous 5 min. As expected, higher titania loading resulted in a smaller intensity value as a result of more light being absorbed. While a higher mass loading is important for the magnitude of the final absorption value, the substrate is also extremely important. The saturation intensity for the 50 mass percent titania films on polycarbonate was determined from an average of three 60 min exposures to hydrogen peroxide gas with concentrations of 72.6, 19.3, and 8.6 ppm and was found to be $42.0 \pm 15.0$. The standard derivation of the saturation intensity of the 50 mass percent titania polycarbonate film is significantly higher than the similar 50 mass percent titania coating on filter paper.

To determine the dependence on peroxide concentration or equivalently the rate of the peroxide flux to the surface, six films on polycarbonate and five coatings on cellulose filter paper were exposed to peroxide concentrations ranging from 0 to 50 ppm. Selected kinetic data can be found in the Supporting Information. Figure 6 shows the phenomenological first-order rate constants, which were determined using the methodology described above, plotted against the measured peroxide concentrations. Experimentally, the error in the measurement was dominated by the small inhomogeneity of the coating. The error bars shown in Figure 6 were estimated first by dividing the films and coatings into four equally sized sections to determine the rate constants for each section and then
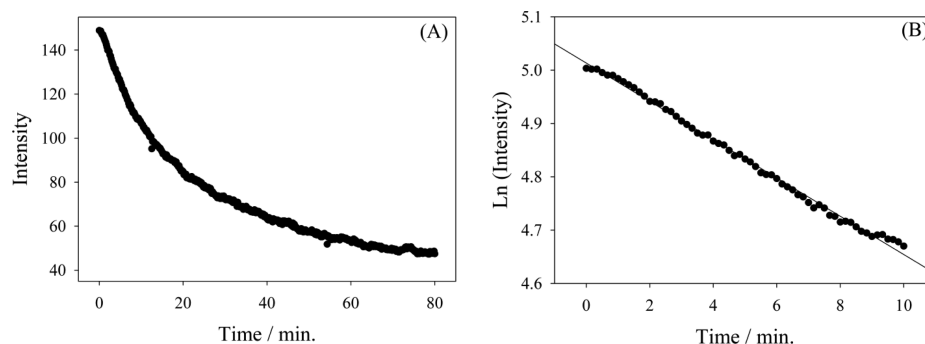
**Figure 5.** (A) Intensity versus exposure time for a 50 mass percent titania coating and (B) the first-order behavior of the first 10 min of exposure. The film was exposed to a peroxide concentration of 43.5 ppm for 40 min.
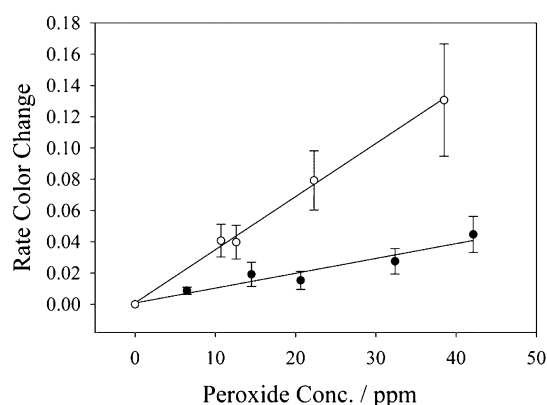


**Figure 6.** Phenomenological first-order rate constants obtained from the 50 mass percent titania films on polycarbonate ($\bullet$) and coatings on filter paper ($\circ$) substrates as a function of the peroxide concentration. Error bars were determined from film homogeneity, as discussed in the text.

computing the standard deviation of the rate constant in each quadrant. The resulting rate constants are linearly dependent on the concentration of peroxide vapor. With a constant concentration of the encapsulated titanium(IV) species within the film, the color change is linearly proportional to the hydrogen peroxide concentration or the flux of hydrogen peroxide molecules to the surface.

The response of both films and coatings to hydrogen peroxide were first order with respect to the gas-phase concentration of hydrogen peroxide. The linear regression of the phenomenological first-order rate constant versus the hydrogen peroxide concentration obtained from the films on polycarbonate and coatings on filter paper were $1.0 \times 10^{-3}$ per ppm with an $R^2$ of 0.98 and $3.4 \times 10^{-3}$ per ppm with an $R^2$ of 1, respectively. These results demonstrate that coatings on cellulose filter paper are over three times as sensitive as the films on polycarbonate, meaning that the filter paper is a superior substrate for both sensitivity and reproducibility. Given that the difference is only a factor of 3 and the surface area and the porosity of the filter paper are significantly greater than those of the polycarbonate substrate, the porous nature of the filter paper is not likely the cause of the different rates. The coating was prepared using a similar amount of the sol−gel precursor solution per unit area as that of the films, eliminating one advantage of a porous substrate. In addition to sensitivity, the background noise for the films and coatings were measured to be 5.2 and 1.1 intensity units, respectively. One major difference between the films and coatings is that the films are

transparent and require a white background material to be placed under the slide, resulting in loss in the reflected intensity. The coatings are white and require no additional background material to reflect the light. Thus, some of the difference between the films and coatings could result from small differences in the experimental setup. Importantly, our measurements show that the chemistry that occurs on these materials is similar. Finally, for higher hydrogen peroxide concentrations, the measured errors for the phenomenological first-order rate constants in Figure 6 were larger than those found for lower concentrations. This was a result of the films and coatings close to the peroxide inlet exhibiting a greater initial rate of coloration.

The effects of titania mass loading on the phenomenological first-order rate constant of the coatings were studied using 0, 25, and 50 mass percent titania mass, where the 0 mass loading was used as a control. Figure 7 shows the response of these coatings to exposures of various peroxide concentrations. Again, select kinetic data can be found in the Supporting Information.
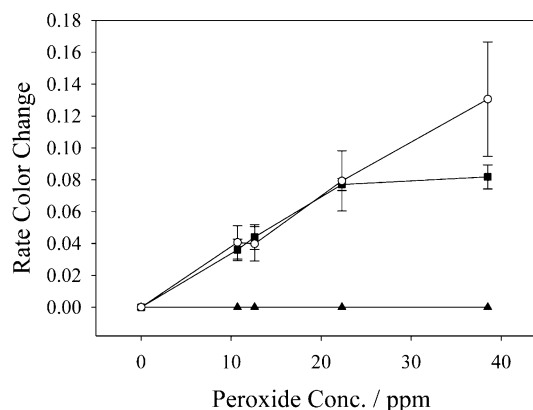


**Figure 7.** Phenomenological first-order rate constants of 0 ($\blacktriangle$), 25 ($\blacksquare$), and 50 ($\circ$) mass percent titania coatings as a function of gas-phase hydrogen peroxide concentration. Error bars were determined from film homogeneity as discussed in the text.

The control films with no titania showed no reactivity toward peroxide. At lower concentrations of hydrogen peroxide vapor (0−25 ppm), the 25% and 50% by mass titania films displayed similar rates of color change at a constant hydrogen peroxide concentration. When exposed to more concentrated vapor, the 25% by mass titania mass loading leveled off to a constant rate of color change independent of the hydrogen peroxide concentration. Leveling off at higher concentrations of

hydrogen peroxide was not observed for the 50% titania coatings, which implies that the rate of intensity change of these films can be used to quantify peroxide concentrations greater than 40 ppm.

**Peroxide Sensitivity and Reaction Mechanism.** The experimental results (Figures 6 and 7) can be qualitatively understood by a reaction mechanism that depends on the flux of hydrogen peroxide to the surface. The phenomenological first-order rate constant at each peroxide concentration appears to depend only on this flux (flux of hydrogen peroxide to the surface). Therefore, the surface reaction rate for the formation of the color species is fast relative to the arrival rate. The final coloration depends only on the concentration of available sites, presumably the encapsulated titanium(IV) species within the film that are completely consumed at later time points. This hypothesis is further supported by the linear dependence of the rate constant on hydrogen peroxide concentration because the flux of hydrogen peroxide molecules to the surface has a linear dependence on the gas-phase concentration or partial pressure. Additionally consistent with this model is the independence of the phenomenological rate constant with titania loading (Figure 7). The fast surface reaction rate implies that, at these peroxide concentrations, the measured rate should be independent of the number of reactive sites within the films and coatings. However, the ultimate capacity of these films is limited by the number of active sites provided by the encapsulated titanium(IV) species; thus, higher loading is associated with greater ultimate color change in the presence of peroxide vapor.

The slope of the phenomenological rate constant versus peroxide concentration (Figures 6 and 7) is an indicator of film and coating sensitivity to peroxide vapor. Color change per parts per million of hydrogen peroxide is directly correlated with film and coating sensitivity to peroxide vapor. In other words, a larger rate color change results in greater sensitivity. By using the concentrations tested herein, the cellulose coatings clearly provided greater sensitivity. A more quantitative estimate was obtained using the slopes and the background noise of the detection system. The background noise for the films and coatings was measured to be 5.2 and 1.1 intensity units, respectively. The major limiting factor is the sensitivity of the web camera. By using $3\sigma$ as an estimate of the limit of detection for the intensity measurements combined with predetermined measurement times, the minimum detectible slope or intensity change was estimated. In turn, the minimum detectible slope was used to identify the detection limit in parts per million. For the 50 mass percent titania films on polycarbonate, the detection limit was estimated to be 90 ppm hydrogen peroxide for a 1 min measurement and 1.5 ppm for a 1 h integration. The coatings on filter paper had a much lower detection limit of 5.4 ppm hydrogen peroxide for a 1 min measurement and 0.09 ppm hydrogen peroxide for a 1 h integration.

## CONCLUSION

Sol−gel methods were used to produce titania in a hydroxypropyl cellulose matrix as films on polycarbonate or coatings on cellulose, with titania/(titania + cellulose) mass percent loading up to 50%. The films on polycarbonate with loadings greater than 50 had a tendency to crack. These films and coatings had reactivity toward hydrogen peroxide and changed color from colorless to an intense yellow when exposed to hydrogen peroxide. By using an inexpensive web camera and a tungsten lamp to measure the reflected light, it

was determined that the films exhibited a first-order behavior with regard to color change when exposed to peroxide vapor concentrations of less than 50 ppm. As the titania content present in the films increased, less light was reflected at saturation. However, the mass ratio in the solution did not affect the response rate for hydrogen peroxide concentrations below 25 ppm. For the 50 mass percent titania films on polycarbonate, the detection limit was estimated to be 90 and 1.5 ppm for a 1 min measurement and a 1 h integration, respectively. The coatings on cellulose provided a 3-fold increase in sensitivity compared to the films on polycarbonate, with a detection limit of 5.4 ppm hydrogen peroxide for a 1 min measurement and 0.09 ppm hydrogen peroxide for a 1 h integration. The major limiting factor was the sensitivity of the web camera. By using a more sensitive detection technique, it may be possible to use the reflected intensity from these films as an extremely sensitive hydrogen peroxide detector. Ongoing studies are being conducted to determine the response of these films to organic peroxides. Nevertheless, a sensor utilizing the titania−cellulose coating may be constructed to monitor peroxide vapor exposure in workplaces to determine whether exposure levels are within the OSHA permissible average exposure limit of 1 ppm of peroxide vapor over an 8 h day.[12]

## ASSOCIATED CONTENT

**Ⓢ Supporting Information**

Measured intensities of 50 mass percent films and coatings illuminated in exposure apparatus with no gas flow and when exposed to water vapor over a 1 h period; additional raw data of the measured intensities and first-order approximations for select films and coatings exposed to peroxide at different concentrations that were used to generate Figures 6 and 7. This material is available free of charge via the Internet at http://pubs.acs.org.

## AUTHOR INFORMATION

**Corresponding Author**

*Phone: (405) 744-8671; fax: (405) 744-6007; e-mail: materer@okstate.edu.

**Notes**

The authors declare no competing financial interest.

## REFERENCES

(1) Carter, H. A. The Chemistry of Paper Preservation Part 2. The Yellowing of Paper and Conservation Bleaching. *J. Chem. Educ.* **1996**, *73*, 1068−1073.

(2) Hage, R.; Lienke, A. Applications of Transition-Metal Catalysts to Textile and Wood-Pulp Bleaching. *Angew. Chem., Int. Ed.* **2006**, *45*, 206−222.

(3) Chen, H.-W.; Chen, C.-Y.; Wang, G.-S. Performance Evaluation of the UV/$H_2O_2$ Process on Selected Nitrogenous Organic Compounds: Reductions of Organic Contents vs. Corresponding C-, N-DBPs Formations. *Chemosphere.* **2011**, *85*, 591−597.

(4) Meneses, M.; Pasqualino, J. C.; Castells, F. Environmental Assessment of Urban Wastewater Reuse: Treatment Alternatives and Applications. *Chemosphere.* **2010**, *81*, 266−272.

(5) Shintani, H. Application of Vapor Phase Hydrogen Peroxide Sterilization to Endoscope. *Biocontrol Sci.* **2009**, *14*, 39−45.

(6) Demirkol, O.; Cagri-Mehmetoglu, A.; Qiang, Z.; Ercal, N.; Adams, C. Impact of Food Disinfection on Beneficial Biothiol Contents in Strawberry. *J. Agric. Food Chem.* **2008**, *56*, 10414−10421.

(7) Qiang, Z.; Demirkol, O.; Ercal, N.; Adams, C. Impact of Food Disinfection on Beneficial Biothiol Contents in Vegetables. *J. Agric. Food Chem.* **2005**, *53*, 9830−9840.

(8) Castle, L.; Mercer, A. J.; Gilbert, J. Chemical Migration from Polypropylene and Polyethylene Aseptic Food Packaging as Affected by Hydrogen Peroxide Sterilization. *J. Food Prot.* **1995**, *58*, 5.

(9) Reidmiller, J. S.; Baldeck, J. D.; Rutherford, G. C.; Marquis, R. E. Characterization of UV-Peroxide Killing of Bacterial Spores. *J. Food Prot.* **2003**, *66*, 8.

(10) Fichet, G.; Antloga, K.; Comoy, E.; Deslys, J. P.; McDonnell, G. Prion Inactivation Using a New Gaseous Hydrogen Peroxide Sterilisation Process. *J. Hosp. Infect.* **2007**, *67*, 278−286.

(11) Pottage, T.; Richardson, C.; Parks, S.; Walker, J. T.; Bennett, A. M. Evaluation of Hydrogen Peroxide Gaseous Disinfection Systems to Decontaminate Viruses. *J. Hosp. Infect.* **2010**, *74*, 55−61.

(12) OSHA. Occupational Safety and Health Standards. https://www.osha.gov/index.html (accessed February 2, 2013).

(13) OSHA. Hydrogen Peroxide. https://www.osha.gov/index.html (accessed February 2, 2013).

(14) OSHA. Chemical Sampling Information: Hydrogen Peroxide. https://www.osha.gov/index.html (accessed September 17, 2013).

(15) Abo, M.; Urano, Y.; Hanaoka, K.; Terai, T.; Komatsu, T.; Nagano, T. Development of a Highly Sensitive Fluorescence Probe for Hydrogen Peroxide. *J. Am. Chem. Soc.* **2011**, *133*, 10629−10637.

(16) Ohta, T.; Yamauchi, Y.; Takitani, S. Fluorometric Determination of Hydrogen Peroxide with Peroxidase and 1-Methyl-1,2,3,4-tetrahydro-$\beta$-carboline-3-carboxylic Acid. *Fresenius' J. Anal. Chem.* **1992**, *343*, 550−552.

(17) Qi, B.; Zhu, Y. Z.; Hu, M.; Zhang, Y.; Tang, X. Fluorometric Determination of Peroxides in an HPLC System. *Anal. Lett.* **2001**, *34*, 1247−1254.

(18) Luo, W.; Li, Y.-S.; Yuan, J.; Zhu, L.; Liu, Z.; Tang, H.; Liu, S. Ultrasensitive Fluorometric Determination of Hydrogen Peroxide and Glucose by Using Multiferroic BiFeO$_3$ Nanoparticles as a Catalyst. *Talanta* **2010**, *81*, 901−907.

(19) Toniolo, R.; Geatti, P.; Bontempelli, G.; Schiavon, G. Amperometric Monitoring of Hydrogen Peroxide in Workplace Atmospheres by Electrodes Supported on Ion-Exchange Membranes. *J. Electroanal. Chem.* **2001**, *514*, 123−128.

(20) Kuwata, S.; Sadaoka, Y. Detection of Gaseous Hydrogen Peroxide Using Planar-Type Amperometric Cell at Room Temperature. *Sens. Actuators, B* **2000**, *65*, 325−326.

(21) Wiedemair, J.; van Dorp, H. D. S.; Olthuis, W.; van den Berg, A. Developing an Amperometric Hydrogen Peroxide Sensor for an Exhaled Breath Analysis System. *Electrophoresis.* **2012**, *33*, 3181−3186.

(22) Kulys, J. Flow-Through Amperometric Sensor for Hydrogen Peroxide Monitoring in Gaseous Media. *Sens. Actuators, B* **1992**, *9*, 143−147.

(23) Lewis, D. The Absorption Spectrum of the Titanium (IV)−Hydrogen Peroxide Complex. *J. Phys. Chem.* **1958**, *62*, 1145−1146.

(24) Possanzini, M.; Di Palo, V. Improved Titanium Method for Determination of Atmospheric H$_2$O$_2$. *Anal. Chim. Acta* **1995**, *315*, 225−230.

(25) Satterfield, C. N.; Bonnell, A. H. Interferences in Titanium Sulfate Method for Hydrogen Peroxide. *Anal. Chem.* **1955**, *27*, 1174−1175.

(26) Matsubara, C.; Kudo, K.; Kawashita, T.; Takamura, K. Spectrophotometric Determination of Hydrogen Peroxide with Titanium 2-((5-Bromopyridyl)azo)-5-(N-propyl-N-sulfopropylamino)Phenol Reagent and Its Application to the Determination of Serum Glucose Using Glucose Oxidase. *Anal. Chem.* **1985**, *57*, 1107−1109.

(27) Huang, H.; Dasgupta, P. K. Renewable Liquid Film-Based Electrochemical Sensor for Gaseous Hydroperoxides. *Talanta* **1997**, *44*, 605−615.

(28) Fujishima, A.; Honda, K. Electrochemical Photolysis of Water at a Semiconductor Electrode. *Nature* **1972**, *238*, 37−38.

(29) O'Regan, B.; Gratzel, M. A Low-Cost, High-Efficiency Solar Cell Based on Dye-Sensitized Colloidal TiO$_2$ Films. *Nature* **1991**, *353*, 737−740.

(30) Lee, S.-H. A.; Abrams, N. M.; Hoertz, P. G.; Barber, G. D.; Halaoui, L. I.; Mallouk, T. E. Coupling of Titania Inverse Opals to Nanocrystalline Titania Layers in Dye-Sensitized Solar Cells†. *J. Phys. Chem. B* **2008**, *112*, 14415−14421.

(31) Chou, T. P.; Zhang, Q.; Russo, B.; Fryxell, G. E.; Cao, G. Titania Particle Size Effect on the Overall Performance of Dye-Sensitized Solar Cells. *J. Phys. Chem. C* **2007**, *111*, 6296−6302.

(32) Nagpal, V. J.; Davis, R. M.; Desu, S. B. Novel Thin Films of Titanium Dioxide Particles Synthesized by a Sol-Gel Process. *J. Mater. Res.* **1995**, *10*, 3068−3078.

(33) Xiao, J.; Chen, W.; Wang, F.; Du, J. Polymer/TiO$_2$ Hybrid Nanoparticles with Highly Effective UV-Screening but Eliminated Photocatalytic Activity. *Macromolecules* **2013**, *46*, 375−383.

(34) Andreozzi, R.; Caprio, V.; Insola, A.; Marotta, R. Advanced Oxidation Processes (AOP) for Water Purification and Recovery. *Catal. Today* **1999**, *53*, 51−59.

(35) Munz, M.; Langridge, M. T.; Devarepally, K. K.; Cox, D. C.; Patel, P.; Martin, N. A.; Vargha, G.; Stolojan, V.; White, S.; Curry, R. J. Facile Synthesis of Titania Nanowires Via a Hot Filament Method and Conductometric Measurement of Their Response to Hydrogen Sulfide Gas. *ACS Appl. Mater. Interfaces* **2013**, *5*, 1197−1205.

(36) Hu, P.; Du, G.; Zhou, W.; Cui, J.; Lin, J.; Liu, H.; Liu, D.; Wang, J.; Chen, S. Enhancement of Ethanol Vapor Sensing of TiO$_2$ Nanobelts by Surface Engineering. *ACS Appl. Mater. Interfaces* **2010**, *2*, 3263−3269.

(37) Gaikwad, V. B.; Jain, G. H. In *Sol-Gel Synthesis of TiO$_2$ Nano Powder and Study of Their Gas Sensing Performance using Thick Film Resistors.* Sensing Technology (ICST), 2011 Fifth International Conference on, Nov 28, 2011−Dec 1, 2011; pp 239−244.

(38) Su, J.; Zou, X.-X.; Zou, Y.-C.; Li, G.-D.; Wang, P.-P.; Chen, J.-S. Porous Titania with Heavily Self-Doped Ti$^{3+}$ for Specific Sensing of CO at Room Temperature. *Inorg. Chem.* **2013**, *52*, 5924−5930.

(39) Tolmachoff, E.; Memarzadeh, S.; Wang, H. Nanoporous Titania Gas Sensing Films Prepared in a Premixed Stagnation Flame. *J. Phys. Chem. C* **2011**, *115*, 21620−21628.

(40) Pan, S. S.; Lu, W.; Zhao, Y. H.; Tong, W.; Li, M.; Jin, L. M.; Choi, J. Y.; Qi, F.; Chen, S. G.; Fei, L. F.; Yu, S. F. Self-Doped Rutile Titania with High Performance for Direct and Ultrafast Assay of H$_2$O$_2$. *ACS Appl. Mater. Interfaces* **2013**, *5*, 12784−12788.

(41) An, W.-J.; Thimsen, E.; Biswas, P. Aerosol-Chemical Vapor Deposition Method for Synthesis of Nanostructured Metal Oxide Thin Films with Controlled Morphology. *J. Phys. Chem. C* **2009**, *1*, 249−253.

(42) Zhang, Y.; Choi, S. W. K.; Puddephatt, R. J. Catalyst Enhanced Chemical Vapor Deposition: Effects on Chemical Vapor Deposition Temperature and Film Purity. *J. Am. Chem. Soc.* **1997**, *119*, 9295−9296.

(43) Qi, Y.; Eskelsen, J. R.; Mazur, U.; Hipps, K. W. Fabrication of Graphene with CuO Islands by Chemical Vapor Deposition. *Langmuir* **2012**, *28*, 3489−3493.

(44) Hendricks, J. H.; Aquino, M. I.; Maslar, J. E.; Zachariah, M. R. Metal and Ceramic Thin Film Growth by Reaction of Alkali Metals with Metal Halides: A New Route for Low-Temperature Chemical Vapor Deposition. *Chem. Mater.* **1998**, *10*, 2221−2229.

(45) Veith, M.; Mathur, S.; Shen, H.; Lecerf, N.; Hüfner, S.; Jilavi, M. H. Single-Step Preparation of Oxide−Oxide Nanocomposites: Chemical Vapor Synthesis of LnAlO$_3$/Al$_2$O$_3$ (Ln = Pr, Nd) Thin Films. *Chem. Mater.* **2001**, *13*, 4041−4052.

(46) Shirman, T.; Freeman, D.; Posner, Y. D.; Feldman, I.; Facchetti, A.; van der Boom, M. E. Assembly of Crystalline Halogen-Bonded Materials by Physical Vapor Deposition. *J. Am. Chem. Soc.* **2008**, *130*, 8162−8163.

(47) Kim, I.-D.; Rothschild, A.; Hyodo, T.; Tuller, H. L. Microsphere Templating as Means of Enhancing Surface Activity and Gas Sensitivity of $CaCu_3Ti_4O_{12}$ Thin Films. *Nano Lett.* **2006**, *6*, 193−198.

(48) Ziehfreund, A.; Maier, W. F. Preparation of Ultrathin Supported Solid Electrolyte Membranes for Oxygen Separation. *Chem. Mater.* **1996**, *8*, 2721−2729.

(49) McFadden, C. F.; Melaragno, P. R.; Davis, J. A. Fabrication of Pyrolytic Carbon Film Electrodes by Pyrolysis of Methane on a Machinable Glass Ceramic. *Anal. Chem.* **1990**, *62*, 742−746.

(50) Çetinörgü, E.; Gümüş, C.; Goldsmith, S.; Mansur, F. Optical and Structural Characteristics of Tin Oxide Thin Films Deposited by Filtered Vacuum Arc and Spray Pyrolysis. *Phys. Status Solidi A* **2007**, *204*, 3278−3285.

(51) Blešić, M. D.; Šaponjić, Z. V.; Nedeljković, J. M.; Uskoković, D. P. $TiO_2$ Films Prepared by Ultrasonic Spray Pyrolysis of Nanosize Precursor. *Mater. Lett.* **2002**, *54*, 298−302.

(52) Seo, I.; Martin, S. W. Structural Properties of Lithium Thio-Germanate Thin Film Electrolytes Grown by Radio Frequency Sputtering. *Inorg. Chem.* **2011**, *50*, 2143−2150.

(53) Zhao, Y.; Zhang, J.; Jiang, D.; Shan, C.; Zhang, Z.; Yao, B.; Zhao, D.; Shen, D. Ultraviolet Photodetector Based on a MgZnO Film Grown by Radio-Frequency Magnetron Sputtering. *ACS Appl. Mater. Interfaces* **2009**, *1*, 2428−2430.

(54) Matolín, V.; Matolínová, I.; Václavů, M.; Khalakhan, I.; Vorokhta, M.; Fiala, R.; Piš, I.; Sofer, Z.; Poltierová-Vejpravová, J.; Mori, T.; Potin, V.; Yoshikawa, H.; Ueda, S.; Kobayashi, K. Platinum-Doped $CeO_2$ Thin Film Catalysts Prepared by Magnetron Sputtering. *Langmuir* **2010**, *26*, 12824−12831.

(55) Oledzka, M.; Lencka, M. M.; Pinceloup, P.; Mikulka-Bolen, K.; McCandlish, L. E.; Riman, R. E. Influence of Precursor on Microstructure and Phase Composition of Epitaxial Hydrothermal $PbZr_{0.7}Ti_{0.3}O_3$ Films. *Chem. Mater.* **2003**, *15*, 1090−1098.

(56) Lagadic, I.; Lacroix, P. G.; Clément, R. Layered MPS3 (M = Mn, Cd) Thin Films as Host Matrixes for Nonlinear Optical Material Processing. *Chem. Mater.* **1997**, *9*, 2004−2012.

(57) Fang, J.; Wang, H.; Xue, Y.; Wang, X.; Lin, T. Magnet-Induced Temporary Superhydrophobic Coatings from One-Pot Synthesized Hydrophobic Magnetic Nanoparticles. *ACS Appl. Mater. Interfaces.* **2010**, *2*, 1449−1455.

(58) Hu, L.; Yoko, T.; Kozuka, H.; Sakka, S. Effects of Solvent on Properties of Sol—Gel-Derived $TiO_2$ Coating Films. *Thin Solid Films.* **1992**, *219*, 18−23.

(59) Mohammadi, M. R.; Cordero-Cabrera, M. C.; Fray, D. J.; Ghorbani, M. Preparation of High Surface Area Titania ($TiO_2$) Films and Powders Using Particulate Sol—Gel Route Aided by Polymeric Fugitive Agents. *Sens. Actuators, B* **2006**, *120*, 86−95.

(60) Smart, L. E.; Moore, E. A. *Solid State Chemistry: An Introduction*, 3rd ed.; CRC Press: Boca Raton, FL, 2005.

(61) Uchiyama, H.; Matsumoto, K.; Kozuka, H. Solvothermal Synthesis of Micron-Sized Spherical Particles in $TiO_2$−$ZrO_2$ Binary System. *J. Cryst. Growth.* **2012**, *338*, 201−207.

(62) Xu, M.; Bunes, B. R.; Zang, L. Paper-Based Vapor Detection of Hydrogen Peroxide: Colorimetric Sensing with Tunable Interface. *ACS Appl. Mater. Interfaces* **2011**, *3*, 642−647.

(63) Kusabe, M.; Kozuka, H.; Abe, S.; Suzuki, H. Sol—Gel Preparation and Properties of Hydroxypropylcellulose—Titania Hybrid Thin Films. *J. Sol-Gel Sci. Technol.* **2007**, *44*, 111−118.

(64) Wiberg, E.; Wiberg, N. *Inorganic Chemistry*; Academic Press: Waltham, MA, 2001.

(65) Schwarzenbach, G.; Muehlebach, J.; Mueller, K. Peroxo Complexes of Titanium. *Inorg. Chem.* **1970**, *9*, 2381−2390.

(66) Mendham, J.; Denney, R. C.; Barnes, J. D.; Thomas, M. J. K. *Vogel's Quantitative Chemical Analysis*, 6th ed.; Prentice Hall: New York, 2000.

(67) Schneider, C. A.; Rasband, W. S.; Eliceiri, K. W. NIH Image to ImageJ: 25 Years of Image Analysis. *Nat. Methods* **2012**, *9*, 671−675.